Carbohydrate Polymers 81 (2010) 394–401

Contents lists available at ScienceDirect

Carbohydrate Polymers

journal homepage: www.elsevier.com/locate/carbpol

Transparent chitosan films reinforced with a high content of nanofibrillated cellulose

Susana C.M. Fernandes[a], Carmen S.R. Freire[a], Armando J.D. Silvestre[a], Carlos Pascoal Neto[a,*], Alessandro Gandini[a], Lars A. Berglund[b], Lennart Salmén[c]

[a] Department of Chemistry and CICECO, Campus de Santiago, University of Aveiro, 3810-193 Aveiro, Portugal
[b] Royal Institute of Technology, Wallenberg Wood Science Center, SE-100 44 Stockholm, Sweden
[c] Innventia AB, Box 5604, SE-114 86 Stockholm, Sweden

ARTICLE INFO

Article history:
Received 20 January 2010
Received in revised form 17 February 2010
Accepted 22 February 2010
Available online 6 March 2010

Keywords:
Chitosan
Water-soluble chitosan
Nanofibrillated cellulose
Transparent films
Nanocomposites
Mechanical and thermal properties

ABSTRACT

This paper reports the preparation and characterization of nanocomposite films based on different chitosan matrices and nanofibrillated cellulose (NFC) for the purpose of improving strength properties. The nanocomposite films were prepared by a simple procedure of casting a water-based suspension of chitosan and NFC, and were characterized by several techniques: namely SEM, X-ray diffraction, visible spectrophotometry, TGA, tensile and dynamic-mechanical analysis. The films obtained were shown to be highly transparent (transmittance varying between 90 and 20% depending on the type of chitosan and NFC content), flexible, displayed better mechanical properties, with a maximum increment on the Young's modulus of 78% and 150% for high molecular weight (HCH) and water-soluble high molecular weight (WSHCH) filled chitosans, respectively; and of 200% and 320% for low molecular weight (LCH) and water-soluble filled (WSLCH) chitosans, respectively. The filled films also showed increased thermal stability, with, for example, an increase in the initial degradation temperature (Td_i) from 227 °C in the unfilled LCH film up to 271 °C in filled LCHNFC50% nanocomposite films, and a maximum degradation temperature (Td_1) raising from 304 °C to 313 °C for the same materials.

1. Introduction

In the last few decades, science and technology has started to move in the direction of renewable raw materials that are environmentally friendly and sustainable. Biopolymers, such as cellulose, chitin, chitosan and starch have been assessed, not only as sustainable resources, but also as attractive materials with interesting properties and functionalities (Gandini and Belgacem, 2008). Biopolymers or their derivatives can be blended with other polymers (including biopolymers) resulting in a number of new composite materials with enhanced properties and applications in several fields. The use of natural cellulose fibres as a reinforcement in polymeric composite materials is an example of this strategy (Wang and Zhang, 2009). More recently, micro and nanofibrillated cellulose (MFC and NFC) substrates have generated a great interest as a reinforcement in composite materials (Nakagaito, Iwamoto, & Yano, 2005; Nakagaito and Yano, 2004, 2005; Yano and Nakahara, 2004) due to their high mechanical performance and to the fact that cellulose is one of the most abundant natural resources. Several studies have been published dealing with the preparation and characterization of micro and nanofibrillated cellulose based-composites with different polymeric matrices, such as poly(vinyl acetate) (Boldizar, Klason, Kubát, Näslund, & Sáha, 1987), hydroxypropyl cellulose (Zimmermann, Pohler, & Geiger, 2004), viscous polysaccharide matrix in the form of a 50/50 amylopectin-glycerol blends (Svagan, Samir, & Berglund, 2007), polylactic acid (Iwatake, Nogi, & Yano, 2008; Suryanegara, Nakagaito, & Yano, 2009), polyvinyl alcohol (Lu, Wang, & Drzal, 2008) and polyurethane (Seydibeyoglu and Oksman, 2008). Chitosan matrices have also been used to produce biodegradable composite films with MFC (diameter of <0.1 μm, length of 100–500 μm) but with the addition of a plasticizer (Hosokawa, Nishiyama, Yoshihara, & Kubo, 1990; Hosokawa, Nishiyama, Yoshihara, Kubo, & Terabe, 1991). However, in this study only a limited number of parameters, such as the effect of the content of chitosan and of the carbonyl content of MFC on the films strength and biodegradability, were evaluated, whereas other relevant composite properties, such as morphology and optical properties, were not considered. More recently, low contents of MFC were also used to enhance the wet properties of chitosan-acetic-acid-salt films (Nordqvist et al., 2007).

Following our interest in the development of new materials based on chitosan (Cunha et al., 2008; Fernandes, Freire et al., 2009; Fernandes, Oliveira et al., 2009; Fernandes, Freire, Pascoal

* Corresponding author. Tel.: +351 234 370693; fax: +351 234 370 084.
E-mail address: cneto@ua.pt (C. Pascoal Neto).

0144-8617/$ – see front matter © 2010 Elsevier Ltd. All rights reserved.
doi:10.1016/j.carbpol.2010.02.037

Neto, & Gandini, 2008) we describe herein the preparation and characterization by several techniques of transparent chitosan films reinforced with high contents (up to 60%) of NFC, using two different chitosan samples, one with a relative low molecular weight and the other with a high molecular weight. The corresponding water-soluble chitosan quaternary ammonium derivatives were also tested in order to avoid the use of acetic acid solutions and consequent films neutralization, thereby increasing the application domains of these materials (e.g. biomedical and coating).

2. Materials and methods

2.1. Materials

Two different chitosan samples (CH) were used, one was kindly provided by Norwegian Chitosan AS (Norway) with relatively low molecular weight (LCH) and the other, with a high molecular weight (HCH) was purchased from Mahtani Chitosan Pvt. Ltd. (India). These two chitosan samples were purified and characterized. The degrees of deacetylation (DDA), determined by ^{1}H NMR (in D_2O containing 1% of CD_3COOD) using a DRX-300 Brüker spectrometer, were found to be 90 and 97% for LCH and HCH, respectively (Desbriéres, Martinez, & Rinaudo, 1996). The viscosity-average molar mass, were 90 000 g/mol for LCH and 350 000 g/mol for HCH, as obtained at 25 °C from a 0.3 M CH_3CO_2H/0.2 M CH_3CO_2Na solution, using the published Mark-Houwink constants (Rinaudo, Milas, & Dung, 1993).

Water-soluble quaternary ammonium derivatives of chitosan were synthesized following the procedure described by Seong, Whang, and Ko (2000). The chitosan derivatives were obtained dissolving 5.0 g of the purified chitosan samples (HCH and LCH) in 250 ml of an aqueous solution of 1% acetic acid and then the glycidyltrimethylammonium chloride (GTMAC-purchased from Fluka, 90% purity) was added while stirring (65 °C for 24 h under a N_2 atmosphere). The ratio of GTMAC/CH molar proportion was 4/1. The obtained water-soluble chitosan (WSCH) derivatives were precipitated and washed with ethanol (purchased from Sigma–Aldrich, 90% purity). The substitution degree of the amino groups was around 30%, as determined by ^{1}H NMR, following a previously described method (Desbriéres et al., 1996).

The nanofibrillated cellulose (NFC) was obtained from L Berglund at KTH in Stockholm, and was prepared according to the procedure described by Henriksson, Henriksson, Berglund, and Lindstrom (2007).

2.2. Methods

2.2.1. Preparation of chitosan/NFC nanocomposites films

Chitosan solutions (1.5%, w/v) were prepared by dissolving CH and WSCH in aqueous acetic acid (1%, v/v) or in water. The NFC contents were varied from 5 to 20% for the CH with a high molecular weight and its water-soluble derivative (WSHCH), and from 5 to 60% in the case of the CH with a relatively low molecular weight and its water-soluble derivative (WSLCH), with respect to the dry weight of chitosan. The maximum amount of NFC used with each type of chitosan was limited by the final viscosity of the ensuing mixtures. The identification of the starting materials and of the prepared nanocomposite films, as well as their global composition in terms of NFC, is shown in Table 1.

The NFC dispersion in the chitosan aqueous solutions was homogenized using an Ultra-Turrax unit for 30 min (20 500 rpm) and then each suspension was degassed to remove entrapped air. Both unfilled CH and chitosan-nanofibrillated cellulose nanocomposite films (CHNFC) were then prepared by casting at 30 °C in a ventilated oven for 16 h, using an acrylic plate (10 × 10 cm^2). Films were removed from the moulds and, before characterization, were kept in a conditioning cabinet at 50% relative humidity (RH) and 25 °C to ensure the stabilization of their moisture content. Prior to testing, the nanocomposites films were stored in a desiccator with phosphorous pentoxide.

Table 1
Identification of the CH-based films.

Sample	CH sample	% of NFC[a]
HCH	High molecular weight	–
HCHNFC5%	High molecular weight	5
HCHNFC10%	High molecular weight	10
HCHNFC20%	High molecular weight	20
LCH	Low molecular weight	–
LCHNFC10%	Low molecular weight	10
LCHNFC20%	Low molecular weight	20
LCHNFC30%	Low molecular weight	30
LCHNFC40%	Low molecular weight	40
LCHNFC50%	Low molecular weight	50
LCHNFC60%	Low molecular weight	60
WSHCH	High molecular weight (water-soluble derivative)	–
WSHCHNFC5%	High molecular weight (water-soluble derivative)	5
WSHCHNFC10%	High molecular weight (water-soluble derivative)	10
WSLCH	Low molecular weight (water-soluble derivative)	–
WSLCHNFC10%	Low molecular weight (water-soluble derivative)	10
WSLCHNFC60%	Low molecular weight (water-soluble derivative)	60

[a] In relation to the oven-dry chitosan mass.

2.2.2. Nanocomposite film characterization

SEM micrographs of the NFC, CH films and of the CHNFC nanocomposite film surfaces were obtained with an HR-FESEM SU-70 Hitachi microscope operating at 1.5 kV.

The X-ray diffraction (XRD) measurements were done with a Philips X'pert MPD diffractometer using Cu Kα radiation.

The transmittance spectra were acquired with a UV–vis Spectrophotometer (Jasco V-560) equipped with a quartz window plate with 16 mm diameter, bearing the holder in the vertical position. Spectra were recorded at room temperature in steps of 1 nm, in the range 400–700 nm.

TGA thermograms were carried out with a Shimadzu TGA 50 analyzer equipped with a platinum cell. Samples were heated at a constant rate of 10 °C/min from room temperature to 800 °C under a nitrogen flow of 20 mL/min. The thermal decomposition temperature was taken at the onset of significant (∼0.5%) weight loss, after the initial moisture and acetic acid (for the LCH and HCH films) losses.

The tensile tests were performed at room conditions on a TA-Hdi Stable Micro Systems Texture Analyser equipped with fixed grips lined with thin rubber at their ends and fitted with a static load cell of 50 N. The film strips were 90 mm long and 10 mm wide. The initial grip separation was set at 50 mm, and the crosshead speed was 0.5 mm/s. Tensile strength, tensile modulus, and elongation to break were calculated using the Instron Series IX software. Fifteen measurements were conducted for each sample (with variability below 5%) and their average values are reported here.

DMA measurements, to study the temperature dependency of the storage modulus, were carried out on a Tritec 2000 DMA Triton equipment operating in the tensile mode. Tests were performed at 1 Hz, an amplitude of 4 μm and a heating rate of 5 °C/min, from

−50 to 165 °C. Test specimens with a typical size of 0.5 mm × 1 mm were used.

DMA measurements, to study the moisture dependency of the storage modulus, were carried out on a Perkin-Elmer DMA7 operating in tension mode. A dynamic deformation was applied at a frequency of 1 Hz. The static load was set to equal 120% of the dynamic load, keeping the amplitude constant at 4 μm. Measurements were performed in humidity scans from 5 to 90% RH after an initial condition at 5% RH for 30 min. The scan rate used was 1% RH/min. The humidity scan was created by a computer controlled humidifier producing humid air by mixing dry and fully saturated air streams. For both DMA techniques, ten measurements (with variability below 5%) were conducted for each sample and their average values are reported here.

3. Results and discussion

3.1. Morphology

SEM micrographs of selected CHNFC nanocomposites films with different NFC contents and chitosan samples are shown in Fig. 1. The random orientation and the good dispersion of the nanofibrillated cellulose in the chitosan matrices were evident, even for the water-soluble chitosan films (WSLCHNFC) with high reinforcement contents. These results are a good indication of the excellent compatibility between the two components of the nanocomposite films that resulted in highly homogeneous materials.

3.2. X-ray diffraction

Fig. 2 shows the X-ray diffractograms of the NFC, unfilled CH samples (LCH, HCH, WSLCH, WSHCH films), and CHNFC nanocomposite films with different NFC contents. The diffractograms of the unfilled HCH and LCH showed the typical X-ray diffraction pattern of chitosan substrates with major peaks at around 2θ of 12 and 19° (Fig. 2a) (Samuels, 1981). The chemical modification of the CH samples with glycidyltrimethylammonium chloride led to an extensive decline of their crystallinity, displaying a diffraction pattern typical of a predominantly amorphous material, as previously observed with other water-soluble chitosan derivatives (Ma et al., 2008). The NFC showed the typical X-ray diffraction profile of Cellulose I (native cellulose), with the main peaks at 2θ of 14.3, 15.9, 22.6 and 33.7° (Fig. 2a) (Hon, 1996). The X-ray diffractograms of all CHNFC nanocomposite films displayed typical diffraction peaks of both polysaccharide components, and, as expected, their intensity is proportional to the content of each polysaccharide. The incorporation of NFC seemed not to affect the crystalinity of the chitosan matrices since no relevant changes on their diffraction profiles were observed (Fig. 2b–d).

3.3. Optical properties

The transparency of the CHNFC films (25–30 μm thick) is illustrated in Fig. 3 for some selected nanocomposites (WSHCH and WSHCHNFC with 5, 10 and 20% of NFC). The constancy in transparency over all the films suggested that the NFC was well dispersed within the CH matrices, as previously observed by SEM. The optical properties of these new materials were also evaluated by measuring their transmittance in the range 400–700 nm (Fig. 4). The transmittance of all CH films, was not affected by the incorporation of 5% of NFC, but for CH films, with NFC contents equal to, or higher than, 10% a reduction in transmittance could be observed, from nearly 90% in CH films down to 20% in some cases. As expected, the transmittance of the CH films decreased with the increase of the NFC content. The difference between the transmittance of the HCH and WSHCH and the LCH and WSLCH films was probably related to the original brownish colour of the LCH sample due to the natural occurrence of coloured impurities (Peniche, Argüelles-Monal, & Goycoolea, 2008). The slightly higher transmittance values obtained for the WSCH derivatives in relation to their corresponding unmodified CH films was probably associated with the chitosan modification procedure, that have implicitly one purification step. The transmittance values of the chitosan substrates studied here were in good agreement with published transmittance data (Larena and Caceres, 2004).

3.4. Thermal properties

The thermal stability and degradation profile of all CH samples and corresponding CHNFC nanocomposite films was assessed

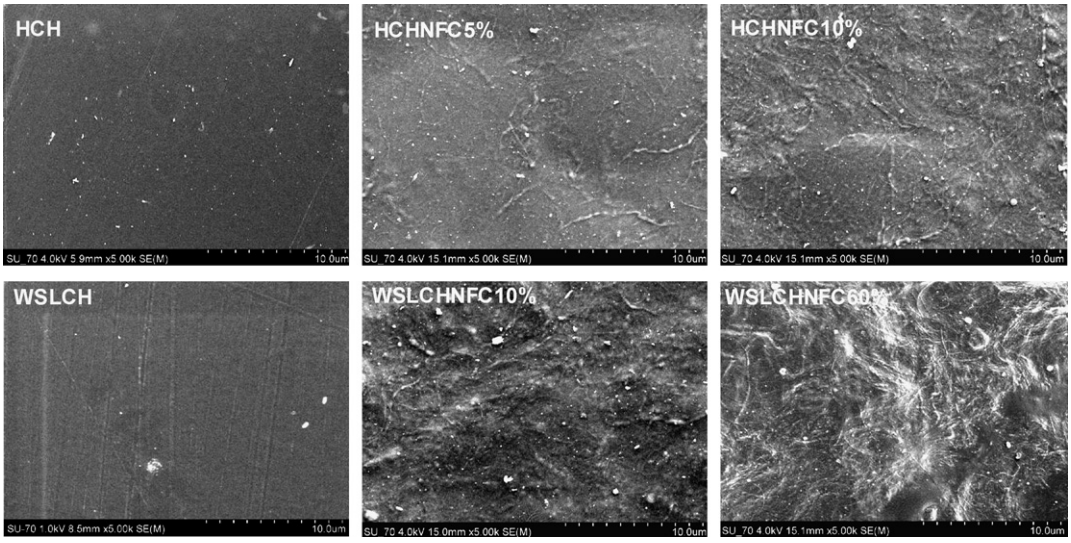

Fig. 1. SEM micrographs of the surface of unfilled HCH and WSLCH film and of some representative HCHNFC and WSLCHNFC nanocomposite films.

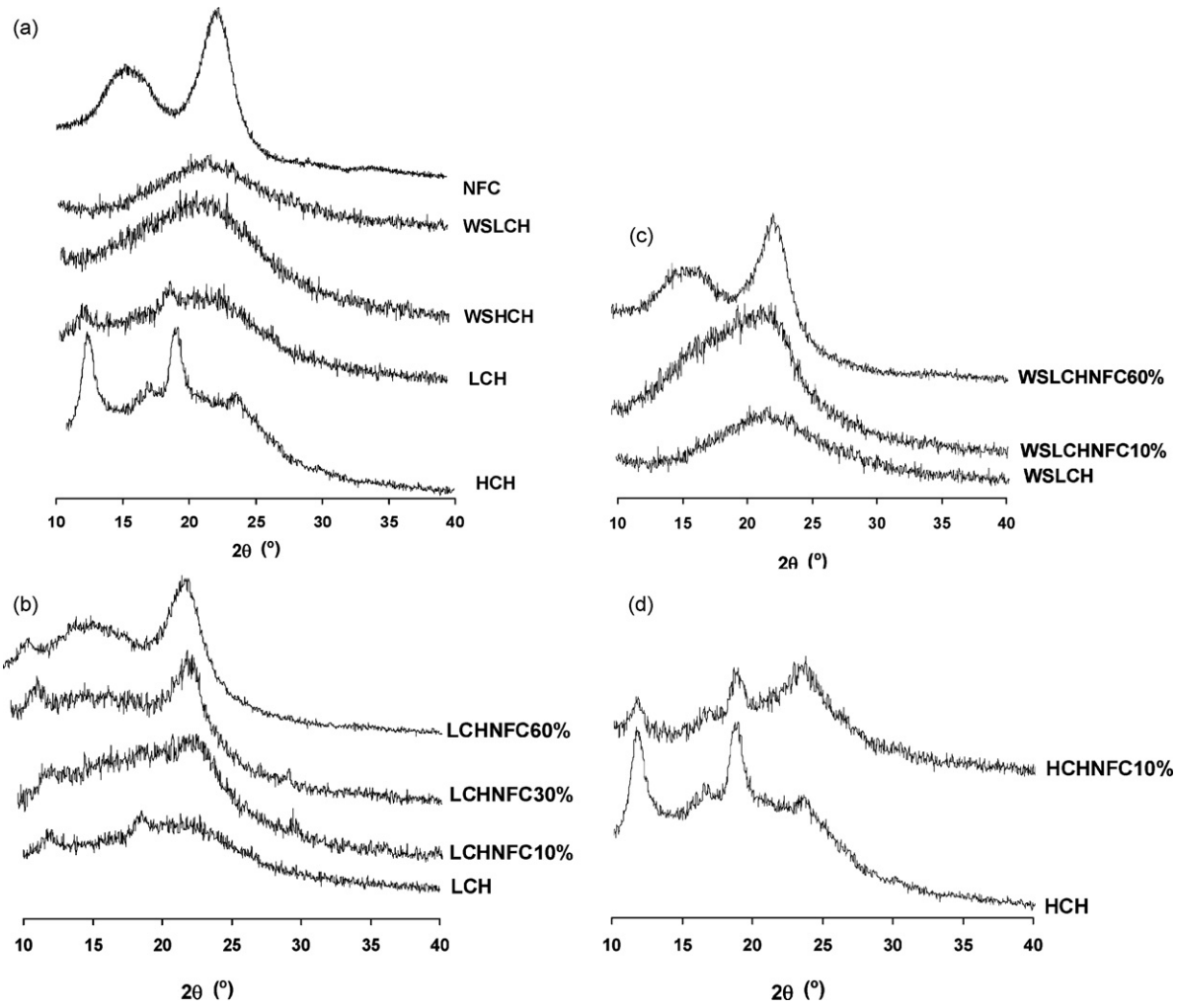

Fig. 2. X-ray diffractograms of (a) NFC and unfilled CH and WSCH films; (b) LCHNFC nanocomposite films; (c) WSLCHNFC nanocomposite films; and (d) HCHNFC nanocomposite films.

by thermogravimetric analysis (Table 2). The thermograms of the HCH and LCH samples showed two mass losses, at around 100° and 200 °C, associated with the volatilization of water and acetic acid, respectively, and a maximum degradation step at around 300 °C (Zohuriaan and Shokrolahi, 2004) assigned to the degradation of chitosan macromolecules. The water-soluble derivatives (WSHCH and WSLCH) were more unstable than their unmodified CH precursors, since they started to decompose at around 180 °C with the maximum degradation step at 260–270 °C. In these cases, the loss of acetic acid was not observed because the films were cast from pure water. On the other hand, NFC displayed a typical double-weight loss profile with the most pronounced degradation step at around 345 °C (Klemm, Philipp, Heinze, Heinze, & Wagenknecht, 1998). The mass loss at around 100 °C, associated with the volatilization of water, was also observed in this situation.

The TGA tracings of the CHNFC nanocomposite films were, in general, a combination of those of the CH and NFC substrates (Table 2). However, the incorporation of NFC into the CH matrices resulted, in most cases, in a considerable increase in the thermal stability (increments of 10–40 °C in the Td_i). Theses results are a good indication of the high compatibility between the two polysaccharide components, resulting in composite materials with enhanced thermal stability. Moreover, the addition of NFC also slightly decreased the water content of the films, particularly in the range of 10–60% of NFC.

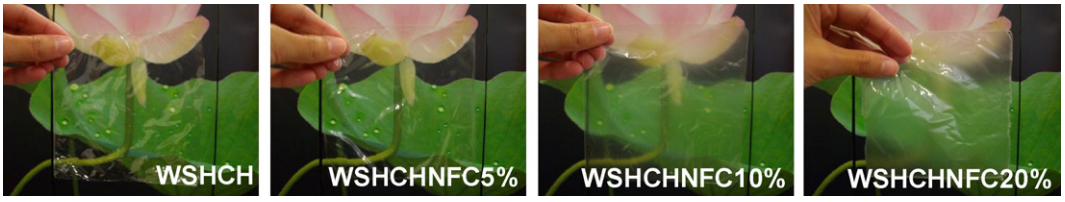

Fig. 3. Images of the WSHCH nanocomposite films containing different percentages of NFC.

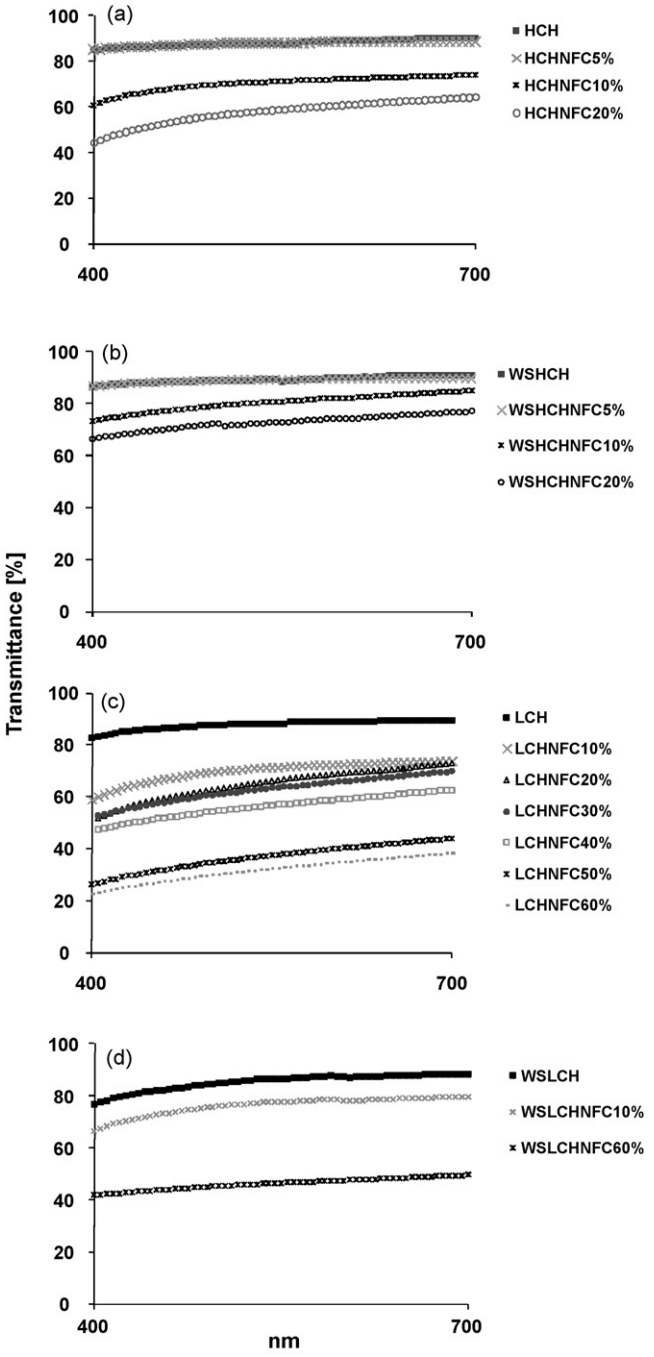

Fig. 4. Transmittance of unfilled CH films and of the corresponding CHNFC and WSCHNFC nanocomposite films with different NFC contents.

Table 2
Thermogravimetric features of the NFC, CH, WSCH, CHNFC and WSCHNFC films.

Sample	Td_i (°C)	Td_1 (°C)	Td_2 (°C)
NFC	240	344(33)[a]	
LCH	227	304(40)	–
LCHNFC10%	271	312(40)	365(53)
LCHNFC20%	269	307(38)	365(53)
LCHNFC30%	270	313(38)	367(54)
LCHNFC40%	273	314(34)	370(51)
LCHNFC50%	271	313(31)	370(51)
LCHNFC60%	246	305(31)	366(51)
WSLCH	193	260(27)	–
WSLCHNFC10%	223	256(37)	301(57)
WSLCHNFC60%	223	297(34)	354(47)
HCH	229	306(40)	–
HCHNFC5%	234	304(45)	350(57)
HCHNFC10%	232	307(40)	364(55)
WSHCH	186	270(31)	–
WSHCHNFC5%	213	277(34)	330(51)
WSHCHNFC10%	194	279(36)	339(53)

[a] Number in parentheses refers to the percentage of decomposition attained at both Td_1 and Td_2. Where Td_i is the initial degradation temperature, Td_1 and Td_2 are the maximum first and second degradation temperatures, respectively.

3.5. Mechanical properties

The reinforcement effect of NFC on the mechanical properties of the CHNFC nanocomposites films was evaluated up to their failure, as a function of the NFC content. Fig. 5(a–c) displays the Young's modulus, the tensile strength and the elongation at break as determined from the typical stress–strain curves of these materials.

The HCH showed a higher Young's modulus than the LCH, confirming that the decrease of the CH degree of polymerization (DP) negatively affected the mechanical performance of the CH films (Chen and Hwa, 1996). The WSCH derivatives displayed the lowest modulus, suggesting that the chemical functionalization with glycidyltrimethyl ammonium chloride clearly affected the mechanical behaviour of CH substrates, obviously associated with the drastic decline of crystallinity previously observed by XRD.

As can be seen in Fig. 5a, the Young's modulus of the CHNFC nanocomposite films increased considerably with the NFC content, keeping constant the relative order of absolute values for the starting chitosans. The maximum amount of NFC used was limited to 20% for HCH and WSHCH, and, in these cases, the maximum increment on the Young's modulus was of 78% and 150%, respectively. However when higher incorporations of NFC were possible, up to 60% in the case of LCH and WSLCH, the increases in the Young's modulus were considerably higher (200% and 320%, respectively). The tensile strength measurements (Fig. 5b) of the studied nanocomposite films were in agreement with the evolution of the Young's modulus. Finally, the incorporation of NFC into the CH matrices caused a significant decrease in the maximum elongation at break, which was proportional to the NFC content. In fact, for quite high NFC loads (40, 50 and 60%), the films became very brittle (Fig. 5c).

The mechanical properties of the CHNFC nanocomposite films were also studied by dynamic-mechanical analysis. Two different experiments were carried out, one to evaluate the effect of the temperature on the dynamic-mechanical behaviour of the materials (varying the temperature from −50 to 165 °C) and another to assess the effect of the humidity (at 30 °C varying the relative humidity from 10 to 80%).

Fig. 6(a–c) shows the temperature dependence of the storage modulus at 1 Hz of CH and some selected CHNFC films. The curves of the storage modulus *vs* temperature of the HCH and LCH showed the two main relaxations, at 0–40 °C and 125–155 °C, typical of CH substrates. The first transition is normally assigned to the β relaxation associated with the hydration of side groups on chitosan (Mucha and Pawlak, 2005) while the transition occurring for higher temperatures, designated as the α relaxation, reflects the glass transition temperature of chitosan (Mucha and Pawlak, 2005). For the water-soluble chitosan derivatives only the β relaxation was observed.

The storage modulus of the LCH films is lower than that of the HCH and the WSCH derivative displayed the lowest storage modulus. The addition of NFC increased considerably the storage modulus in the entire temperature range, and did not affect the

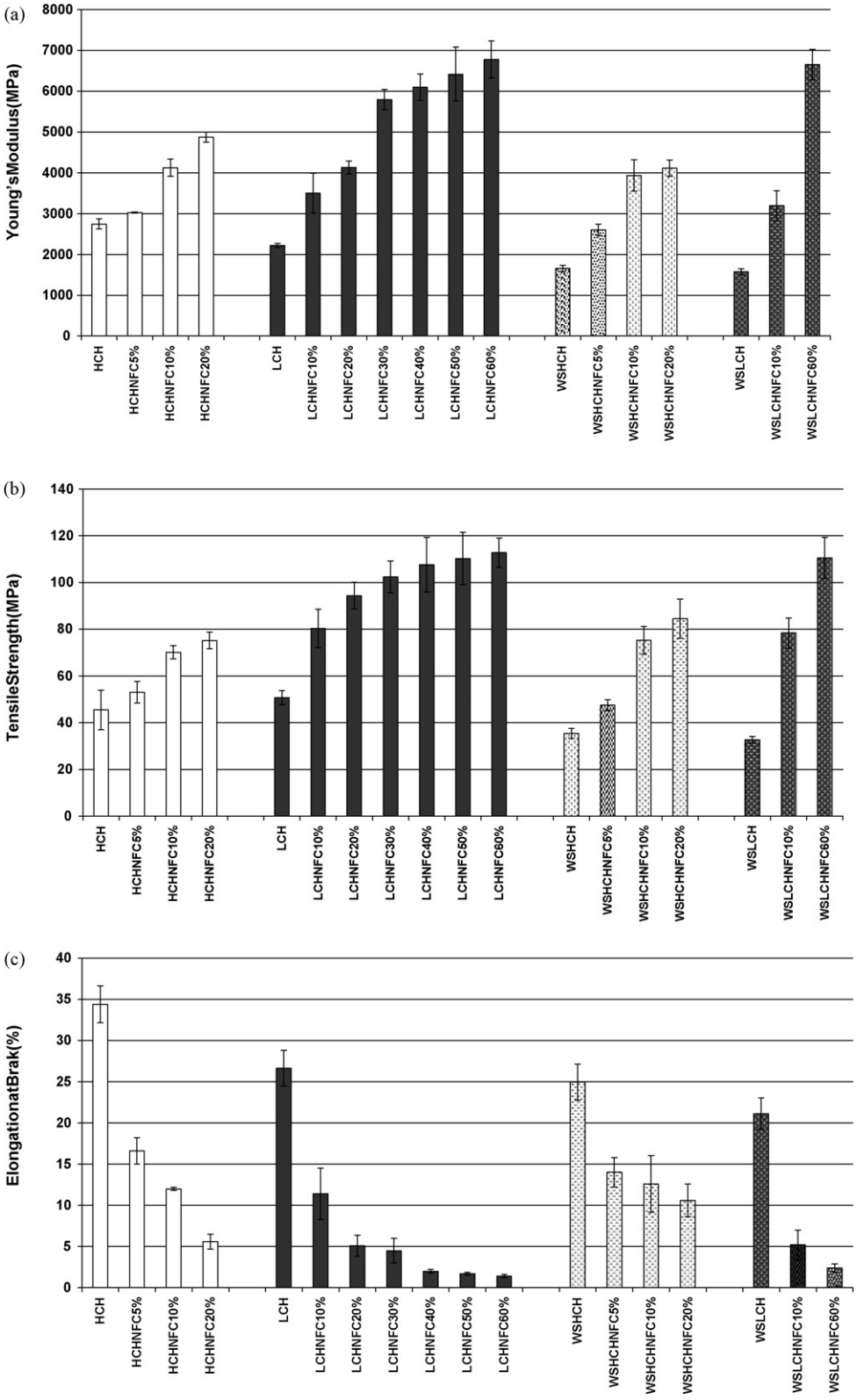

Fig. 5. Young's modulus, tensile strength and elongation to break of the CH samples and the corresponding nanocomposite films with different NFC contents.

main transitions of chitosan, as illustrated by the LCH and WSLCH films (Fig. 6b and c). These results are in excellent agreement with the tensile experiments.

Fig. 7(a–c) illustrates the effect of the relative humidity on the dynamic-mechanical properties of CH films and the corresponding CHNFC nanocomposite films. As can be seen in Fig. 7a, the CH and WSCH films showed quite different behaviours with respect to the stiffness development with increasing humidity. Both the CH and WSCH films showed a decrease of the storage modulus with the relative humidity. However, the WSCH films displayed a more significant reduction at low humidity values due to their high moisture sensitivity related to the incorporation of the qua-

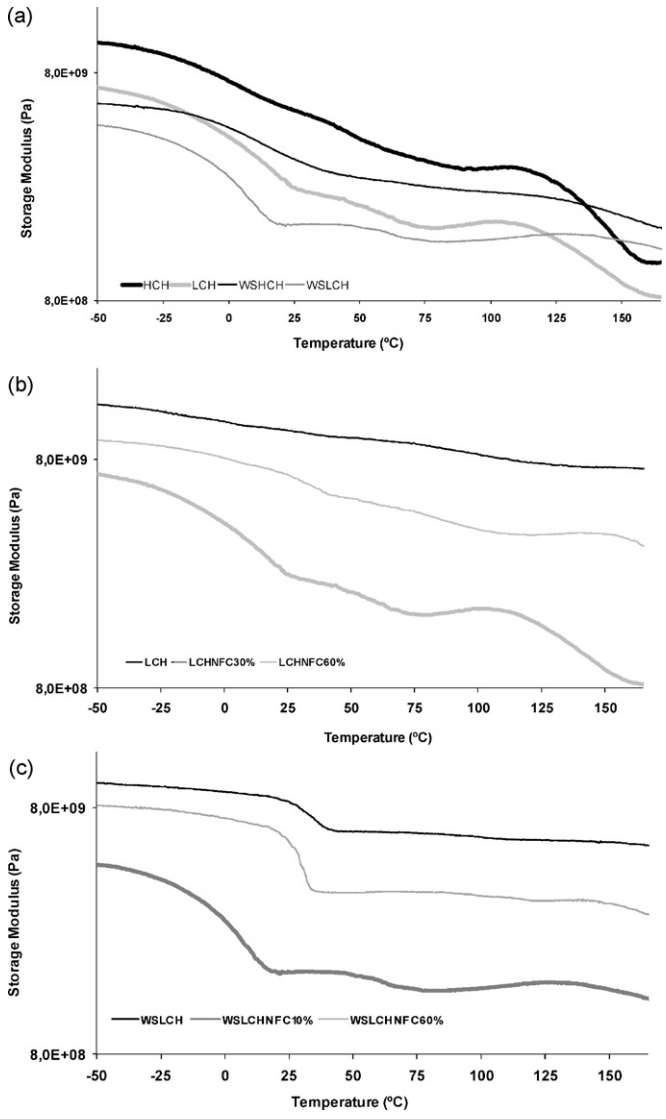

Fig. 6. Temperature dependency of the storage modulus of (a) CH and WSCH films; (b) LCH nanocomposite films; and (c) WSLCH nanocomposite films.

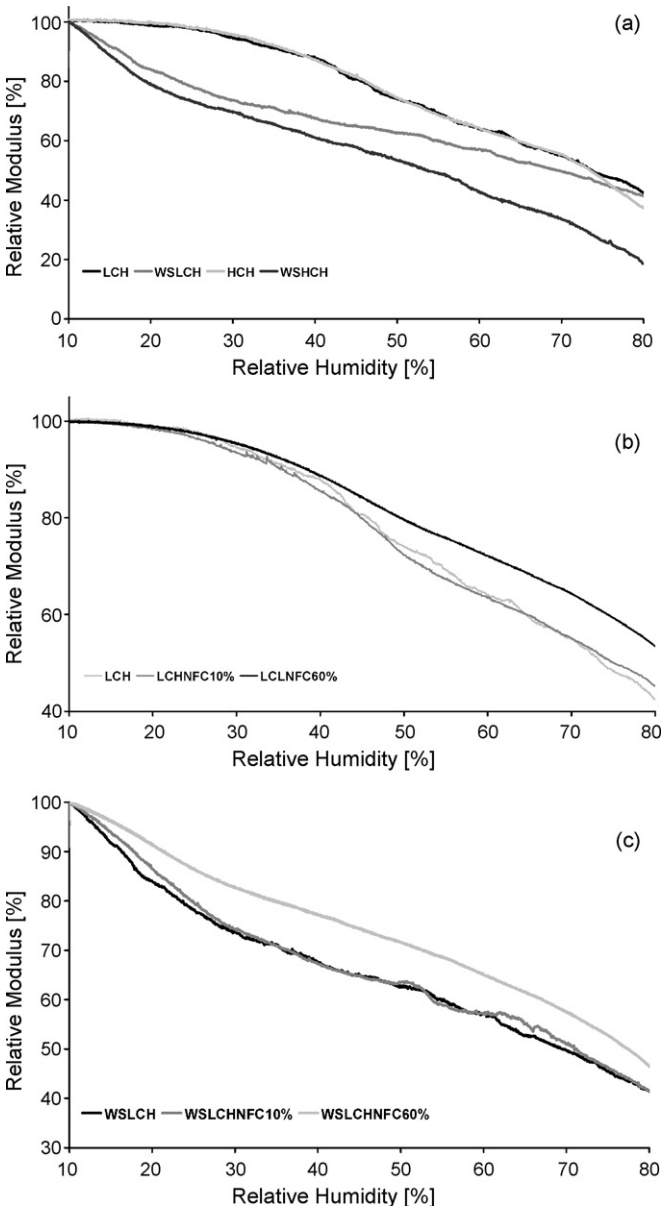

Fig. 7. Moisture dependence of the relative modulus at 30 °C for (a) CH and WSCH films; (b) LCHNFC nanocomposite films; and (c) WSLCHNFC nanocomposite films.

ternary ammonium. The softening behaviour of the CH and WSCH nanocomposite films was not affected by the incorporation of 10% of NFC. For contents higher than 10% an improved moisture resistance was observed.

The enhancement of the mechanical and thermo-mechanical properties of CH films by the incorporation of NFC, confirmed the strong adhesion and interactions between the two polysaccharide components that carries out from their similar chemical structures and the nano fibrillar structure of NFC. These results are in excellent agreement with previous works reporting on the incorporation of MFC and NFC into several polymeric matrices, such as PLA, PVA and starch, among others (Iwatake et al., 2008; Lu et al., 2008; Nordqvist et al., 2007; Suryanegara et al., 2009; Svagan et al., 2007).

Globally the properties of CHNFC nanocomposite films are better than those demonstrated by similar chitosan films reinforced with bacterial cellulose nanofibrils that we reported recently (Fernandes, Oliveira et al., 2009). This behaviour could be due to the better dispersion of NFC into the chitosan matrices, as well as to the higher aspect ratio (i.e., the ration between average length and the diameter of the fibres) of the NFC compared with bacterial cellulose (Azeredo, 2009).

4. Conclusion

Transparent chitosan-nanofribrillated cellulose composite films were prepared by simply casting water (or 1% acetic solutions) suspensions of chitosan with different contents of NFC (up to 60%). The transparency (transmittance varying between 90 and 20% depending on the type of chitosan and NFC content) indicates that the dispersion of the NFC into the chitosan matrices was quite good. These materials were in general very homogenous, flexible and presented better mechanical (with a maximum increment of Young's modulus of 150% for WSHCH and of 320% for WSLCH filled samples) and thermo-mechanical properties (storage modulus of LCHNFC10% films increase 24% and 90% in the case of LCHNFC60% films compared to LCH films at 25 °C) than the corresponding unfilled chitosan films. The thermal stability of the chitosan films also increased considerably with the incorporation of the NFC. Their prominent properties could be exploited for several applications, such as in transparent functional packaging, electronic devices and biomedical applications.

The higher molar mass chitosans showed higher elongation at break than lower molar mass chitosans (with values of elongation at break of 34% and 27% for HCH and LCH films, respectively; and of 30% and 21% for their, respectively, water-soluble derivatives, WSHCH and WSLCH), also with NFC reinforcement (varying, using 10% of NFC content for example, between 12% for HCH and 5% for WSLCH). With NFC addition to the chitosans, tensile strength and modulus were completely dominated by the NFC network. The nanocomposites prepared with the high-DP water-soluble chitosan are particularly interesting for future studies, since they have an attractive combination of properties, including high optical transparency.

Acknowledgements

The authors thank Norwegian Chitosan AS. (Norway) for their generous gift of chitosan (LCH). Anne-Mari Olsson at Innventia AB and Sandra Magina at CICECO-University of Aveiro are gratefully acknowledged for help with the DMA measurements, moisture scan equipment and temperature scan equipment, respectively. Susana Fernandes thank the Fundação para a Ciência e a Tecnologia (FCT) for her Scientific Research grant (SFRH/BD/41388/2007) and the Peter Wallenberg's Foundation for support her stay in Stockholm. Lennart Salmén thanks the Biomime Center for its financial support. The authors also thank FCT for the funding within the scope of the "National Program for Scientific re-equipment", Rede/1509/RME/2005 and REEQ/515/CTM/2005.

References

Azeredo, H. M. C. (2009). Nanocomposites for food packaging applications. *Food Research International*, *42*, 1240–1253.

Boldizar, A., Klason, C., Kubát, J., Näslund, P., & Sáha, P. (1987). Prehydrolyzed cellulose as reinforcing filler for thermoplastics. *International Journal of Polymers Materials*, *11*, 229–262.

Chen, R. H., & Hwa, H. D. (1996). Effect of molecular weight of chitosan with the same degree of deacetylation on the thermal, mechanical, and permeability properties of the prepared membrane. *Carbohydrate Polymers*, *29*, 353–358.

Cunha, A. G., Fernandes, S. C. M., Freire, C. S. R., Silvestre, A. J. D., Pascoal Neto, C., & Gandini, A. (2008). What is the real value of chitosan's surface energy? *Biomacromolecules*, *9*, 610–614.

Desbriéres, J., Martinez, C., & Rinaudo, M. (1996). Hydrophobic derivatives of chitosan: Characterization and rheological behaviour. *International Journal of Biological Macromolecules*, *19*, 21–28.

Fernandes, S. C. M., Freire, C. S. R., Pascoal Neto, C., & Gandini, A. (2008). The bulk oxypropilation of chitin and chitosan and the characterization of the ensuing polyols. *Green Chemistry*, *10*, 93–97.

Fernandes, S. C. M., Freire, C. S. R., Silvestre, A. J. D., Pascoal Neto, C., Gandini, A., Desbriéres, J., et al. (2009). A study of the distribution of chitosan onto and within a paper sheet using a fluorescent chitosan derivative. *Carbohydrates Polymers*, *78*, 760–766.

Fernandes, S. C. M., Oliveira, A. L., Freire, C. S. R., Silvestre, A. J. D., Pascoal Neto, C., Gandini, A., et al. (2009). Novel transparent nanocomposite films based on chitosan and bacterial cellulose. *Green Chemistry*, *11*, 2023–2029.

Gandini, A., & Belgacem, M. N. (2008). In M. N. Belgacem, & A. Gandini (Eds.), *Monomers, polymers and composites from renewable resources* (pp. 1–16). London, U.K.: Elsevier.

Henriksson, M., Henriksson, G., Berglund, L. A., & Lindstrom, T. (2007). An environmentally friendly method for enzyme-assisted preparation of microfibrillated cellulose (MFC) nanofibers. *European Polymer Journal*, *43*, 3434–3441.

Hon, D. N.-S. (1996). *Chemical modification of lignocellulosic materials*. New York: Marcel Dekker.

Hosokawa, J., Nishiyama, M., Yoshihara, K., & Kubo, T. (1990). Biodegradable film derived from chitosan and homogenized cellulose. *Industrial & Engineering Chemistry Research*, *29*, 800–805.

Hosokawa, J., Nishiyama, M., Yoshihara, K., Kubo, T., & Terabe, A. (1991). Reaction between chitosan and cellulose on biodegradable composite film formation. *Industrial & Engineering Chemistry Research*, *30*, 788–792.

Iwatake, A., Nogi, M., & Yano, H. (2008). Cellulose nanofiber-reinforced polylactic acid. *Composites Science and Technology*, *68*, 2103–2106.

Klemm, D., Philipp, B., Heinze, T., Heinze, U., & Wagenknecht, W. (1998). *Comprehensive cellulose chemistry* Weinheim: Wiley-VCH.

Larena, A., & Caceres, D. A. (2004). Variability between chitosan membrane surface characteristics as function of its composition and environmental conditions. *Applied Surface Science*, *238*, 273–277.

Lu, J., Wang, T., & Drzal, T. (2008). Preparation and properties of microfibrillated cellulose polyvinyl alcohol composite materials. *Composites: Part A*, *39*, 738–746.

Ma, G., Yang, D., Zhou, Y., Xiao, M., Kennedy, J. F., & Nie, J. (2008). Preparation and characterization of water-soluble N-alkylated chitosan. *Carbohydrate Polymers*, *74*, 121–126.

Mucha, M., & Pawlak, A. (2005). Thermal analysis of chitosan and its blends. *Thermochimica Acta*, *427*, 69–76.

Nakagaito, A. N., Iwamoto, S., & Yano, H. (2005). Novel high-strength biocomposites based on microfibrillated cellulose having nanoorder-unit web-like network structure. *Applied Physics A*, *80*(1), 93–97.

Nakagaito, A. N., & Yano, H. (2004). The effect of morphological changes from pulp fiber towards nano-scale fibrillated cellulose on the mechanical properties of high-strength plant fiber based composites. *Applied Physics A*, *78*(4), 547–552.

Nakagaito, A. N., & Yano, H. (2005). Bacterial cellulose: The ultimate nano-scalar cellulose morphology for the production of high-strength composites. *Applied Physics A*, *80*(1), 155–159.

Nordqvist, D., Idermark, J., Hedenqvist, M., Gällstedt, M., Ankerfors, M., & Lindström, T. (2007). Enhancement of the wet properties of transparent chitosan-acetic acid-salt films using microfibrillated cellulose. *Biomacromolecules*, *8*, 2398–2403.

Peniche, C., Argüelles-Monal, W., & Goycoolea, F. M. (2008). In M. N. Belgacem, & A. Gandini (Eds.), *Monomers, polymers and composites from renewable resources* (pp. 517–542). London, U.K.: Elsevier.

Rinaudo, M., Milas, M., & Dung, L. P. (1993). Characterization of chitosan. Influence of ionic strength and degree of acetylation on chain expansion. *International Journal of Biological Macromolecules*, *15*, 281–285.

Samuels, R. J. (1981). Solid state characterization of the structure of chitosan films. *Journal of Polymers Science Part B-Polymers Physics*, *19*, 1081–1105.

Seong, H. S., Whang, H. S., & Ko, S. W. (2000). Synthesis of a quaternary ammonium derivative of chito-oligosaccharide as antimicrobial agent for cellulosic fibers. *Journal of Applied Polymers Science*, *76*, 2009–2015.

Seydibeyoglu, M. Ö., & Oksman, K. (2008). Novel nanocomposites based on polyurethane and micro fibrillated cellulose. *Composites Science Technology*, *68*, 908–914.

Suryanegara, L., Nakagaito, A., & Yano, H. (2009). The effect of crystallization of PLA on the thermal and mechanical properties of microfibrillated cellulose-reinforced PLA composites. *Composites Science Technology*, *69*, 1187–1192.

Svagan, A. J., Samir, M. A. S. A., & Berglund, L. A. (2007). Biomimetic polysaccharide nanocomposites of high cellulose content and high toughness. *Biomacromolecules*, *8*, 2556–2563.

Wang, Y., & Zhang, L. (2009). In L. Yu (Ed.), *Biodegradable polymer blends and composites from renewable resources* (pp. 129–161). New Jersey: Wiley. Part I, Chapter 6.

Yano, H., & Nakahara, S. (2004). Bio-composites produced from plant microfiber bundles with a nanometer unit web-like network. *Journal of Material Science*, *39*(5), 1635–1638.

Zimmermann, T., Pohler, E., & Geiger, T. (2004). Cellulose fibrils for polymer reinforcement. *Advanced engineering materials*, *6*(9), 754–761.

Zohuriaan, M. J., & Shokrolahi, F. (2004). Thermal studies on natural and modified gums. *Polymer Test*, *23*, 575–579.